International Journal Of

Recent Scientific Research

ISSN: 0976-3031

Volume: 7(4) April -2016

MOLECULAR STRUCTURE, MOLECULAR DOCKING, VIBRATIONAL SPECTRA, NBO, AND UV-VISIBLE ANALYSIS OF KETOTIFEN BY DFT METHOD

Solaichamy R and Karpagam J

THE OFFICIAL PUBLICATION OF
INTERNATIONAL JOURNAL OF RECENT SCIENTIFIC RESEARCH (IJRSR)
http://www.recentscientific.com/ recentscientific@gmail.com

ISSN: 0976-3031

Available Online at http://www.recentscientific.com

International Journal of Recent Scientific Research
Vol. 7, Issue, 4, pp. 9840-9849, April, 2016

International Journal of Recent Scientific Research

Research Article

MOLECULAR STRUCTURE, MOLECULAR DOCKING, VIBRATIONAL SPECTRA, NBO, AND UV-VISIBLE ANALYSIS OF KETOTIFEN BY DFT METHOD

Solaichamy R and Karpagam J*

Department of Physics (Engineering.), Annamalai University, Annamalainagar- 608 002, Tamil Nadu, India

ARTICLE INFO

Article History:

Received 05th January, 2015
Received in revised form 08th February, 2016
Accepted 10th March, 2016
Published online 28st April, 2016

Keywords:

FT-IR; FT-Raman; NBO; UV-Vis; TED; Molecular Docking.

ABSTRACT

The Fourier transform infrared (4000–400 cm^{-1}) and Fourier transform Raman (3500–50 cm^{-1}) spectra of Ketotifen were recorded and analyzed. The equilibrium geometry, bonding features and harmonic vibrational wavenumbers were investigated with the help of density functional theory (DFT) method using B3LYP/6-31G (d,p) as basis set. The observed vibrational wavenumbers were compared with the calculated results. Natural bond orbital analysis confirms the presence of intramolecular charge transfer and the hydrogen bonding interaction. Predicted electronic absorption spectra from TD-DFT calculation have been analyzed comparing with the UV–Vis (200–800 nm) spectrum. The HOMO–LUMO energy gap explains the charge interaction taking place within the molecule. The Chemical reactivity and chemical potential of Ketotifen is calculated. In addition, molecular electrostatic potential (MEP), analysis were investigated using theoretical calculations.

INTRODUCTION

Ketotifen (KT) 4-(1-Methylpiperidin-4-ylidene)-4,9-dihydro-10H-benzo[4,5]cyclohepta [1,2-b]thiophen-10-one has been widely use as an antiallergic and antianaphylactic agent in adults and children in the treatment of bronchial asthma and allergic diseases [Grant, Goa, Fitton, & Sorkin, 1990]. It is an antihistamine that inhibits release of inflammatory mediators derived from mast cells (MC).

By this way, ketotifen can prevent local tissue damage and multiorgan dysfunction due to vasoactive and proinflammatory mediators derived from MC after intestinal ischemia/ reperfusion it can also preclude the mesenteric alterations and splanchnic inflammatory changes related to acute portal hypertension in rats. Ketotifen has also investigated in multidrug resistance in human breast cancer cells and doxorubicin toxicity in mice. Several delivery systems have been designed to modulate ketotifen delivery by different routes of administration Due to its use in the treatment of bronchial asthma, particularly of an allergic origin, dry powder inhalation formulations of liposomally entrapped drug have been prepared for direct ketotifen delivery in the respiratory tract [Sandra Guerrero *et al*., 2010].

Experimental

FT-IR, FT-Raman and UV–Vis spectral measurements

The compound Ketotifen was purchased from Aldrich chemicals, USA. The FT-IR spectrum of Ketotifen compound was recorded in the range of 4000–400 cm^{-1} on a BRUKER Optik GmbH FT-IR spectrometer using KBr pellet technique. The spectrum was recorded in the room temperature, with scanning speed of 10 cm^{-1}, and spectral resolution: 4 cm^{-1}. FT-Raman spectrum of the title compound was recorded using 1064 nm line of Nd:YAG laser as excitation wavelength in the region 3500–50 cm^{-1} on a BRUKER RFS 27: FT-Raman Spectrometer equipped with FT-Raman molecule accessory. The spectral resolution was set to 2 cm^{-1} in back scattering mode. The laser output was kept at 150mW for the solid sample. The ultraviolet absorption spectra of Ketotifen were examined in the range 200–800 nm using Cary 500 UV–VIS–NIR spectrometer. The UV pattern is taken from a 10 to 5 M solution of Ketotifen, dissolved in ethanol solvent. The theoretically predicted IR and Raman spectra at B3LYP/6-31G(d,p) level calculation along with experimental FT-IR and FT-Raman spectra are shown in Figs. 1 and 2. The FT-IR and UV–Vis spectral measurements were carried out at St. Josephs College Trichy and FT-Raman spectral measurement was carried out at Indian Institute of Technology (IIT), Chennai.

*Corresponding author: **Karpagam J***
Department of Physics (Engineering.), Annamalai University, Annamalainagar- 608 002, Tamil Nadu, India

COMPUTATIONAL DETAILS

The density functional theory DFT/B3LYP with the 6-31G(d,p) as basis set was adopted to calculate the properties of Ketotifen in the present work. All the calculations were performed using Gaussian 03W program package [3] with the default convergence criteria without any constraint on the geometry [4]. The assignments of the calculated wavenumbers are aided by the animation option of Gauss View 3.0 graphical interface for Gaussian programs, which gives a visual presentation of the shape of the vibrational modes along with available related molecules [5]. Furthermore, theoretical vibrational spectra of the title compound were interpreted by means of TED using the VEDA 4 program [6]. The optimized structural parameters were used in the vibrational frequency calculations at DFT levels to characterize all stationary points as minima. As the hybrid B3LYP functional tends to overestimate the fundamental normal modes of vibration, the computed frequencies were scaled with appropriate values to bring harmonization between the theoretical and experimental wavenumbers [7]. Vibrational frequencies were computed at DFT level which had reliable one-to-one correspondence with experimental IR and Raman frequencies [8]. The Natural Bond Orbital (NBO) calculations were performed using NBO 3.1 program [9] as implemented in the Gaussian 03W [3] package at the DFT/B3LYP level; in order to understand various second order interactions between filled orbital of one subsystem and vacant orbital of another subsystem which is a measure of the intermolecular delocalization or hyper conjugation.

Prediction of Raman intensities

The Raman activities (S_{Ra}) calculated with Gaussian 03W program Wallingford CT, [2004] converted to relative Raman intensities (I_{Ra}) using the following relationship derived from the intensity theory of Raman scattering [Sutton, 1958]

$$I_i = \frac{f(v_o - v_i)^4 S_i}{v_i[1 - \exp(-hcv_i / kt)]}$$

Where, v_0 is the laser exciting wavenumber in cm^{-1} (in this work, we have used the excitation wavenumber $v_0 = 9398.5\ cm^{-1}$, which corresponds to the wavelength of 1064 nm of a Nd-YAG laser), v_i the vibrational wavenumber of the i^{th} normal mode (cm^{-1}) while S_i is the Raman scattering activity of the normal mode v_i [Solaichamy *et al*., 2016].

Docking Studies

The molecular structure of protein (PDB ID: 1ZMS) was taken from RCSB Protein Data Bank, http://www.rcsb.org/pdb [12]. Initial structures of Ketotifen were generated by ChemBioOffice 2008. The geometries of Ketotifen legand were subsequently optimized at DFT/B3LYP/ 6-31G (d,p) by Gaussian 03 [3]. The molecular modeling docking calculations of Ketotifen legand with 1ZMS protein were carried out by means of the Autodock tools (ADT) v1.5.4 [13] and Autodock 4.2.3 program from the Scripps Research Institute. In docking study, the search was extended over the whole receptor Ketotifen used as blind docking. The grid maps were generated with 0.375 Å spaces using a grid box of 70–70–70 Å. The search was carried out with the Lamarckian Genetic Algorithm because it has been pointed out to be most efficient, reliable and successful methods in Autodock [14]. The docking parameters used were as follows: GA population size = 150; maximum number of energy evaluation = 25,00,000 and others used were default parameters. The docking conformation with the lowest binding free energy was used for further analysis by Molegro Molecular Viewer software from http:// www.clcbio.com/products/molegro/.

RESULTS AND DISCUSSIONS

Structural Analysis

The optimized geometric parameters such as bond lengths, bond angles and dihedral angles of the title molecule were given in Table 1 using DFT calculation with 6-31G(d,p) as a basis set. The atom numbering scheme adopted in this study is given in Fig. 1. To the best of our knowledge, experimental data on the geometric structure of the title molecule are not available till date in the literature. Therefore, the theoretical results of KT have been molecule 4-(1-Methylpiperidin-4-ylidene)-4, 9-dihydro-10H-benzo [4, 5] cyclohepta [1, 2-b] thiophen-10-one as given in Table 1**.** The C-C bond length of the thiophen ring varies from 1.370 Å-1.392 Å. Due to the C-H group substitution on the C3, and $C4^{th}$ position of the thiophen ring, the C-C bond lengths are not same for example C1-C2=1.392 Å, C1-C10=1.468 Å C2-C3=1.431 Å, C1-C6=1.487 Å, C3-C4=1.370 Å calculated by DFT method.

The C-S bond length on the thiophen ring varies from 1.747 Å -1.724 Å by DFT method is good agreement theoretical value. The C10-O15 bond length is 1.224 Å calculated by DFT method. N-C bond lengths are N16-C17=1.464 Å, N16-C21=1.476 Å, and N16-C22=1.453 Å calculated by DFT respectively, this result shows good agreement Theoretical values. The C-H bond lengths of Methyl (CH_3) group is C9-H25=1.099 Å, C9-H26=1.092 Å, C17-H31=1.097 Å, C17-H32=1.109 Å, C18-H33=1.100 Å, C18-H34=1.093 Å, C20-H35=1.091 Å, C20-H36=1.100 Å, C21-H37=1.095 Å, C21-H38=1.100 Å, C22-H39=1.094 Å, C22-H40=1.108 Å, and C22-H41=1.096 Å calculated by DFT method.

As shown in Fig. 1, the molecular structure of title compound contains one six-membered ring this ring (C7-C8-C11-C12-C13-C14) adopt chair conformations. The bond angle at point on the substitution is C7-C8-C11=119.4° calculated by DFT respectively. The unit – N16-C17-C18–C19- connected with C6 by the way of an equatorial bond, and the angles of C2-C6-C19=122.7° (DFT), C7-C6-C19=122.7° (DFT), C6-C19-C18 show 123.8° (DFT), and C6-C19-C20 show 123.4° (DFT) like a bridge that aligned with the molecules.

Dihedral angles of Cycloheptatriene part are found as C1-C2-C6-C7=48.31°, C10-C1-C2-C6=5.11°, C2-C6-C7-C8=-64.33°, C6-C7-C8-C9=-0.75°, C7-C8-C9-C10=70.02°, and C8-C9-C10-C1=-56.11°. From the theoretical values, we found the idea most of our optimized bond lengths are slightly larger than experimental values due to be able to fact that the theoretical calculations belong to be able to isolated molecules throughout gaseous phase as well as the experimental results belong for molecules in the solid state. Dihedral angles of Benzoic ring is C8-C7-C14-C13=-1.10°, C7-C8-C11-C12=-0.11°, C8-C11-

C12-C13=-0.50°, C11-C12-C13-C14=0.31°, and C12-C13-C14-C7=0.49° respectively.

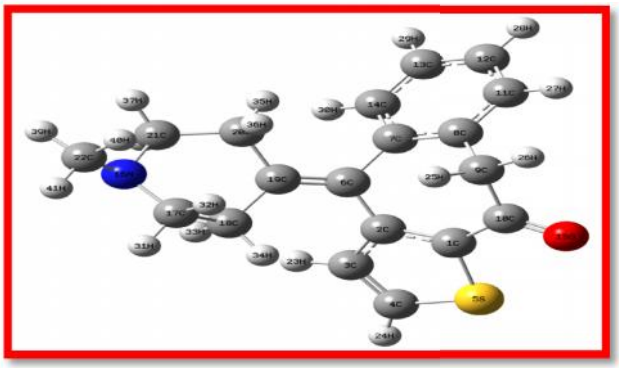

Fig.1 Optimized Molecular structure and atomic numbering of Ketotifen

Table 1 Comparison of experimental and theoretical optimized parameter values of the Ketotifen [bond length in (A˚), angles in (◦)].

Bond length	B3LYP	Bond angle	B3LYP	Dihedral angle	B3LYP
C1-C2	1.392	C2-C1-S5	112.0	S5-C1-C2-C3	-0.26
C1-S5	1.747	C2-C1-C10	130.1	S5-C1-C2-C6	-177.15
C1-C10	1.468	S5-C1-C10	117.9	C10-C1-C2-C3	-178.00
C2-C3	1.431	C1-C2-C3	111.3	C10-C1-C2-C6	5.11
C2-C6	1.487	C1-C2-C6	124.3	C2-C1-S5-C4	0.24
C3-C4	1.370	C3-C2-C6	124.4	C10-C1-S5-C4	178.29
C3-H23	1.083	C2-C3-C4	113.2	C2-C1-C10-C9	-0.60
C4-S5	1.724	C2-C3-H23	123.3	C2-C1-C10-O15	178.38
C4-H24	1.082	C4-C3-H23	123.4	S5-C1-C10-C9	-178.23
C6-C7	1.501	C3-C4-S5	112.5	S5-C1-C10-O15	0.75
C6-C19	1.354	C3-C4-H24	127.3	C1-C2-C3-C4	0.15
C7-C8	1.408	S5-C4-H24	120.1	C1-C2-C3-H23	-178.02
C7-C14	1.401	C1-S5-C4	91.0	C6-C2-C3-C4	177.03
C8-C9	1.514	C2-C6-C7	114.6	C6-C2-C3-H23	-1.14
C8-C11	1.399	C2-C6-C19	122.7	C1-C2-C6-C7	48.31
C9-C10	1.531	C7-C6-C19	122.7	C1-C2-C6-C19	-130.71
C9-H25	1.099	C6-C7-C8	119.7	C3-C2-C6-C7	-128.18
C9-H26	1.092	C6-C7-C14	121.1	C3-C2-C6-C19	52.80
C10-O15	1.224	C8-C7-C14	119.1	C2-C3-C4-S5	0.04
C11-C12	1.395	C7-C8-C9	119.9	C2-C3-C4-H24	-179.17
C11-H27	1.087	C7-C8-C11	119.4	H23-C3-C4-S5	178.20
C12-C13	1.394	C9-C8-C11	120.7	H23-C3-C4-H24	-1.00
C12-H28	1.086	C8-C9-C10	113.3	C3-C4-S5-C1	-0.16
C13-C14	1.395	C8-C9-H25	109.6	H24-C4-S5-C1	179.11
C13-H29	1.086	C8-C9-H26	111.4	C2-C6-C7-C8	-64.33
C14-H30	1.086	C10-C9-H25	107.5	C2-C6-C7-C14	112.93
N16-C17	1.464	C10-C9-H26	106.6	C19-C6-C7-C8	114.68
N16-C21	1.476	H25-C9-H26	108.2	C19-C6-C7-C14	-68.06
N16-C22	1.453	C1-C10-C9	117.5	C2-C6-C19-C18	0.92
C17-C18	1.532	C1-C10-O15	121.3	C2-C6-C19-C20	177.06
C17-H31	1.097	C9-C10-O15	121.1	C7-C6-C19-C18	-178.01
C17-H32	1.109	C8-C11-C12	121.0	C7-C6-C19-C20	-1.87
C18-C19	1.520	C8-C11-H27	119.1	C6-C7-C8-C9	-0.75
C18-H33	1.100	C12-C11-H27	119.9	C6-C7-C8-C11	178.21
C18-H34	1.093	C11-C12-C13	119.7	C14-C7-C8-C9	-178.06
C19-C20	1.519	C11-C12-H28	119.9	C14-C7-C8-C11	0.90
C20-C21	1.538	C13-C12-H28	120.3	C6-C7-C14-C13	-178.37
C20-H35	1.091	C12-C13-C14	119.8	C6-C7-C14-H30	0.83
C20-H36	1.100	C12-C13-H29	120.3	C8-C7-C14-C13	-1.10
C21-H37	1.095	C14-C13-H29	119.9	C8-C7-C14-H30	178.11
C21-H38	1.100	C7-C14-C13	121.0	C7-C8-C9-C10	70.02
C22-H39	1.094	C7-C14-H30	119.0	C7-C8-C9-H25	-50.11
C22-H40	1.108	C13-C14-H30	120.0	C7-C8-C9-H26	-169.84
C22-H41	1.096	C17-N16-C21	113.6	C11-C8-C9-C10	-108.93
		C17-N16-C22	111.5	C11-C8-C9-H25	130.94
		C21-N16-C22	114.2	C11-C8-C9-H26	11.22
		N16-C17-C18	111.2	C7-C8-C11-C12	-0.11
		N16-C17-H31	108.6	C7-C8-C11-H27	179.90
		N16-C17-H32	112.1	C9-C8-C11-C12	178.84

Table 1 (Cont) Comparison of experimental and theoretical optimized parameter values of the Ketotifen [bond length in (A˚), angles in (◦)].

Bond length	B3LYP	Bond angle	B3LYP	Dihedral angle	B3LYP
		C18-C17-H31	109.8	C9-C8-C11-H27	-1.15
		C18-C17-H32	108.7	C8-C9-C10-C1	-56.11
		H31-C17-H32	106.3	C8-C9-C10-O15	124.92
		C17-C18-C19	111.1	H25-C9-C10-C1	65.20
		C17-C18-H33	107.7	H25-C9-C10-O15	-113.78
		C17-C18-H34	110.0	H26-C9-C10-C1	-178.95
		C19-C18-H33	110.0	H26-C9-C10-O15	2.07
		C19-C18-H34	111.3	C8-C11-C12-C13	-0.50
		H33-C18-H34	106.6	C8-C11-C12-H28	-179.99
		C6-C19-C18	123.8	H27-C11-C12-C13	179.49
		C6-C19-C20	123.4	H27-C11-C12-H28	0.00
		C18-C19-C20	112.6	C11-C12-C13-C14	0.31
		C19-C20-C21	110.9	C11-C12-C13-H29	-179.10
		C19-C20-H35	111.9	H28-C12-C13-C14	179.80
		C19-C20-H36	108.8	H28-C12-C13-H29	0.38
		C21-C20-H35	110.3	C12-C13-C14-C7	0.49
		C21-C20-H36	108.8	C12-C13-C14-H30	-178.70
		H35-C20-H36	106.0	H29-C13-C14-C7	179.91
		N16-C21-C20	113.8	H29-C13-C14-H30	0.71
		N16-C21-H37	108.9	C21-N16-C17-C18	-37.13
		N16-C21-H38	109.4	C21-N16-C17-H31	-158.02
		C20-C21-H37	109.5	C21-N16-C17-H32	84.84
		C20-C21-H38	108.7	C22-N16-C17-C18	-167.92
		H37-C21-H38	106.3	C22-N16-C17-H31	71.19
		N16-C22-H39	110.2	C22-N16-C17-H32	-45.95
		N16-C22-H40	114.0	C17-N16-C21-C20	-22.08
		N16-C22-H41	109.4	C17-N16-C21-H37	-144.44
		H39-C22-H40	108.1	C17-N16-C21-H38	99.71
		H39-C22-H41	107.6	C22-N16-C21-C20	107.39
		H40-C22-H41	107.4	C22-N16-C21-H37	-14.97
				C22-N16-C21-H38	-130.83
				C17-N16-C22-H39	-173.63
				C17-N16-C22-H40	64.61
				C17-N16-C22-H41	-55.57
				C21-N16-C22-H39	55.89
				C21-N16-C22-H40	-65.87
				C21-N16-C22-H41	173.95
				N16-C17-C18-C19	63.97
				N16-C17-C18-H33	-56.53
				N16-C17-C18-H34	-172.37
				H31-C17-C18-C19	-175.84
				H31-C17-C18-H33	63.65
				H31-C17-C18-H34	-52.18
				H32- C17-C18-C19	-59.95
				H32- C17-C18-H33	179.54
				H32- C17-C18-H34	63.71
				C17-C18-C19-C6	150.09
				C17-C18-C19-C20	-26.42
				H33-C18-C19-C6	-90.73
				H33-C18-C19-C20	92.76
				H34-C18-C19-C6	27.19
				H34-C18-C19-C20	-149.32
				C6-C19-C20-C21	153.02
				C6-C19-C20-H35	29.49
				C6-C19-C20-H36	-87.28
				C18-C19-C20-C21	-30.45
				C18-C19-C20-H35	-153.98
				C18-C19-C20-H36	89.24
				C19-C20-C21-N16	58.31
				C19-C20-C21-H37	-179.64
				C19-C20-C21-H38	-63.89
				H35-C20-C21-N16	-177.24
				H35-C20-C21-H37	-55.20
				H35-C20-C21-H38	60.55
				H36-C20-C21-N16	-61.37
				H36-C20-C21-H37	60.68
				H36-C20-C21-H38	176.43

Vibrational Assignments

The theoretical vibrational analysis of the compound KT is analyzed using DFT/B3LYP 6-31G (d,p) method. The observed and calculated FT-IR, FT-Raman spectrum of title molecules is given in Fig. 2 and Fig. 3. The values are tabulated in Table 2. The Ketotifen molecule consists of 41 atoms, which undergoes 117 normal modes of vibrations. Which include 41 stretching, 38 bending and 38 torsional modes of vibration. The optimized geometry of compound KT is located at the minima on the potential energy state. The calculated vibrational frequencies are found to be in good agreement with the observed FT-IR frequencies. The theoretical vibrational frequencies obtained for compound Ketotifen is interpreted by means of Total energy distribution (TED %) calculations using VEDA4 method. The normal modes assignment of the theoretical frequencies is visualized and substantiated with the help of the GaussView 5.0 visualization program. The molecule KT belongs to C1 symmetry. All the modes are IR active modes. The significant normal modes with TED (10%) are given in order of decreasing wave numbers in Table 2.

Thiophen ring vibration

Thiophene is considered aromatic, although theoretical calculations suggest that the degree of aromaticity is less than that of benzene. The "electron pairs" on sulfur are significantly delocalized in the pi electron system. As a consequence of its aromaticity, thiophene does not exhibit the properties seen for conventional thioethers [16, 17]. The C-C stretching vibration of the Thiophen ring observed the FT-IR band at 1387 cm^{-1}, and FT-Raman band at 476 cm^{-1} and the computed scaled wavenumbers at 1498, 1397, 1367, 1245, 998, 478, and 304 cm^{-1} by DFT method. These modes are good agreement with literature assigned C-C-C in-plane bending vibration at 829 cm^{-1} by DFT method. This is good agreement with Thiophen derivatives [18].

Methylene group vibrations

For the assignments of CH_2 group frequencies, basically six fundamentals vibration can be associated to each CH_2 group namely, CH_2 symmetric stretch, antisymmetric stretch, scissoring and rocking modes, which belong to polarized in-plane vibrations . In addition to that, wagging and twisting mode of CH_2 group would be expected to be depolarized for out-of-plane bending vibration. The asymmetric CH_2 stretching vibration generally observed in the region 3000–2900 cm^{-1}, while the CH_2 symmetric stretch will appear between 2900 cm^{-1} and 2800 cm^{-1} [19]. For title molecule CH_2 anti symmetric and symmetric stretching vibrations observed at 2980, 2927, 2900 cm^{-1} and 2979, 2890 cm^{-1} in FT-IR and FT-Raman spectrum respectively. The computed wavenumbers at 3006, 2990, 2929 and 2900 cm^{-1} are assigned as CH_2 anti symmetric and symmetric stretching vibrations. The CH_2 scissoring vibrations appear normally in the region 1490–1435 cm^{-1} as medium intense bands [20]. In our present investigation FT-Raman band at 1462 cm^{-1} and computed wavenumbers at 1463, 1458 and 1431 have been identified as CH_2 scissoring vibrations. Absorption of hydrocarbons due to CH_2 twisting and wagging vibration is observed in the 1350-1150 cm^{-1} region [21]. For title molecule the FT-IR band at 1343, 1261cm^{-1} by DFT calculation gives the CH_2 twisting vibrations.

C-N vibrations

Silverstein *et al*., (1991) assigned the C-N stretching absorption in the region 1382 to 1286 cm^{-1} for aromatic amines. For title molecule C-N stretching vibration observed at 1343 and 1261 cm^{-1} in FT-IR spectrum and 1336 and 1263 cm^{-1} in FT-Raman spectrum. The calculated wave numbers at 1339, 1266 and 1258 cm^{-1} has been identified as C-N stretching vibration, which is good agreement with experimental values. The calculated scaled wavenumber at 513 cm^{-1} by DFT method gives CNC in-plane bending vibrations. The observed FT-Raman band at 355 cm^{-1} and computed wave number at 308 cm^{-1} has been identified as CCCN out-of plane bending vibration.

C-O and C-S Vibrations

The C–O stretching vibration in Cycloheptatriene occurs as a strongest band in the region 1700 to 1300 cm^{-1}. For title molecule C-O stretching vibration observed at 1651 cm^{-1} in FT-IR spectrum. The calculated wavenumbers by DFT method at 1681 cm^{-1} assigned C-O stretching vibrations. The C–S-C in-plane-bending vibration in Thiophene ring is 632 cm^{-1} in FT-IR spectrum respectively. For title molecule C-S-C in-plane-bending vibration vibration observed at 681 and 644 cm^{-1} by DFT method respectively. The observed FT-Raman band at 443 cm^{-1} and theoretically predicted wavenumbers at 437 cm^{-1} are identified as C-S-C in-plane bending vibrations.

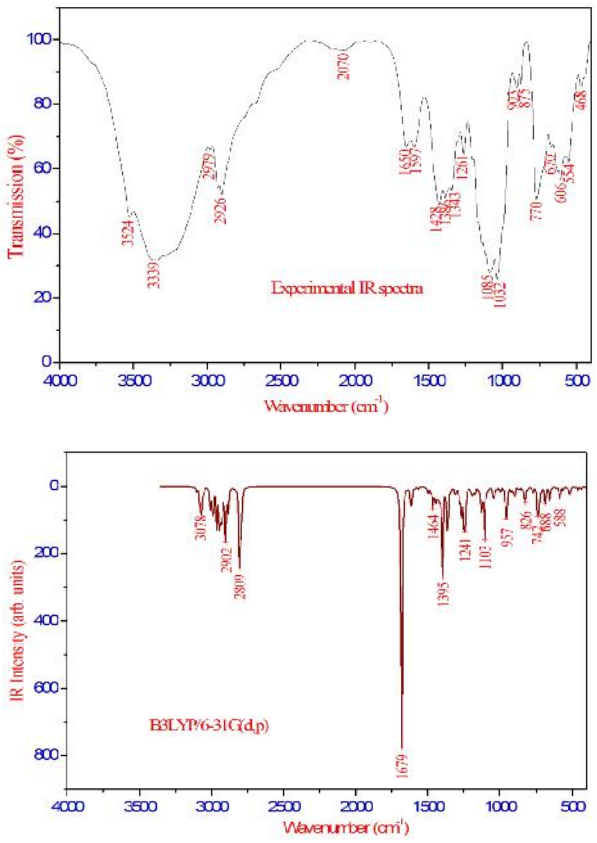

Fig.2 Comparison of experimental and theoretical B3LYP/6-31G(d,p) FT-IR spectrum for Ketotifen

Table 2 Comparison of the experimental and calculated vibrational spectra and proposed assignments of Ketotifen

Mode No	Experimental wave numbers/cm^{-1}		Theoretical wave numbers/cm^{-1}				Vibrational assignments with PED (≥10%)
	FT-IR	FT-Raman	B3LYP/6-31G(d,p) Unscaled	scaled	I_{IR} [a]	I_{Ra} [b]	
1			3260	3132	0.51	8.43	$\nu_{C4H24(90)}$
2		3118	3229	3103	3.72	2.30	$\nu_{C3H23(90)}$
3			3207	3081	25.30	13.74	$\nu_{C12H28(83)}$
4			3195	3069	22.87	3.39	$\nu_{C11H27(99)}$
5			3184	3059	3.32	4.90	$\nu_{C11H27(82)}$
6			3178	3053	2.63	1.10	$\nu_{C11H27(99)}$
7			3131	3008	8.50	3.62	$\nu_{C9H26(92)}$
8			3129	3006	14.52	3.23	$\nu_{C20H35(97)}$
9			3112	2990	32.11	5.71	$\nu_{C22H39(94)}$
10	2980	2979	3109	2987	9.70	2.42	$\nu_{C18H34(94)}$
11			3083	2963	33.63	5.74	$\nu_{C21H37(90)}$
12			3065	2944	55.83	6.72	$\nu_{C22H39(93)}$
13	2927		3048	2929	48.19	7.60	$\nu_{C17H31(94)}$
14			3031	2912	9.87	4.00	$\nu_{C9H25(92)}$
15			3022	2903	37.12	3.65	$\nu_{C18H33(82)}$
16	2900		3018	2900	15.92	3.67	$\nu_{C18H33(79)}$
17		2890	3003	2885	22.21	6.26	$\nu_{C20H36(98)}$
18			2921	2806	115.07	6.02	$\nu_{C22H40(91)}$
19			2906	2792	42.36	1.57	$\nu_{C17H32(94)}$
20	1651		1750	1681	277.73	12.25	$\nu_{O15C10(90)}$
21			1680	1614	30.61	88.12	$\nu_{C6C19(73)}$
22	1597		1654	1589	1.70	7.85	$\nu_{C7C14(60)}+\delta_{H27C11C12(14)}$
23			1627	1563	1.84	3.31	$\nu_{C11C12(53)}+\delta_{C7C14C13(12)}$
24			1559	1498	8.02	14.47	$\nu_{C1C2(72)}$
25			1540	1480	4.41	4.32	$\delta_{H31C17H32(71)}$
26			1524	1464	2.03	2.68	$\delta_{H37C21H38(78)}$
27		1462	1523	1463	15.79	1.48	$\delta_{H27C11C12(45)}$
28			1518	1458	3.40	2.97	$\delta_{H39C22H40(80)}+\gamma_{C22H39N16H40(12)}$
29			1503	1444	18.47	5.03	$\delta_{H39C22H40(80)}+\gamma_{C22H39N16H41(14)}$
30	1429		1490	1431	7.89	0.30	$\nu_{C11C12(26)}+\delta_{H28C12C13(46)}$
31			1484	1426	2.43	1.42	$\delta_{H35C20H36(85)}$
32			1479	1421	7.64	2.07	$\delta_{H33C18H34(78)}$
33			1473	1415	0.96	4.33	$\delta_{H39C22H40(70)}+\tau_{H31C17N16C21(11)}$
34			1472	1414	9.21	3.20	$\delta_{H25C9H26(77)}$
35	1387		1454	1397	91.74	32.27	$\nu_{C1C2(68)}$
36			1423	1367	13.47	10.17	$\nu_{C2C3(40)}+\delta_{H23C3C4(25)}$
37			1417	1361	50.07	1.47	$\tau_{H31C17N16C21(51)}$
38	1343	1336	1394	1339	3.89	1.87	$\tau_{H31C17N16C21(64)}$
39			1365	1311	4.82	1.82	$\delta_{H37C21C20(10)}+\tau_{H33C18C19C20(35)}$
40			1356	1303	3.31	4.23	$\nu_{C18C19(14)}+\delta_{H37C21C20(24)}+\tau_{H33C18C19C20(17)}$
41			1351	1298	0.22	1.19	$\nu_{C7C14(45)}+\tau_{H26C9C10C1(11)}$
42			1332	1280	9.55	1.40	$\delta_{H27C11C12(12)}$
43			1327	1275	4.03	5.54	$\delta_{H31C17N16(11)}+\gamma_{C21C20N16H38(12)}$
44		1263	1318	1266	24.78	1.61	$\nu_{N16C17(15)}+\delta_{H33C18C19(10)}+\gamma_{C22H39N16H40(19)}$
45	1261		1310	1258	6.87	10.66	$\delta_{H23C3C4(13)}$
46			1296	1245	62.24	0.53	$\nu_{C1C2(24)}+\delta_{H27C11C12(10)}$
47			1287	1237	17.77	6.81	$\delta_{H25C9C8(37)}$
48			1247	1198	6.13	7.59	$\delta_{H31C17N16(24)}+\tau_{H33C18C19C20(11)}$
49			1241	1192	1.08	15.56	$\delta_{H35C20C19(30)}$
50			1233	1185	9.01	8.23	$\delta_{H33C18C19(26)}$
51			1220	1172	5.14	7.85	$\nu_{C8C9(16)}$
52			1197	1150	1.84	1.22	$\nu_{C11C12(12)}+\delta_{H28C12C13(11)}$
53			1189	1143	0.02	2.83	$\nu_{C11C12(17)}+\delta_{H27C11C12(81)}$
54			1183	1136	1.97	0.57	$\nu_{C18C19(31)}$
55		1128	1173	1127	21.00	4.72	$\tau_{H26C9C10C1(26)}$
56			1161	1115	11.85	2.36	$\nu_{N16C17(21)}+\delta_{H37C21C20(17)}+\gamma_{C22H39N16H41(26)}$
57			1147	1102	44.13	2.13	$\nu_{N16C17(23)}+\gamma_{C22H39N16H41(40)}$
58	1086	1087	1128	1084	3.32	4.96	$\delta_{H24C4C3(64)}$
59			1119	1075	1.33	5.68	$\nu_{C11C12(19)}+\delta_{H28C12C13(14)}$
60		1048	1089	1046	10.24	1.72	$\nu_{C17C18(36)}+\gamma_{C22H39N16H40(19)}$
61			1080	1037	10.60	0.89	$\gamma_{C20C6C18C19(13)}$
62	1032		1073	1030	1.93	9.04	$\nu_{C11C12(54)}+\delta_{H27C11C12(21)}$
63			1060	1018	1.54	4.07	$\nu_{C20C21(33)}+\gamma_{C21C20N16H38(14)}$
64			1038	998	5.44	5.12	$\nu_{C2C3(12)}$
65			1005	966	8.41	2.87	$\nu_{N16C17(16)}+\gamma_{C21C20N16H38(10)}$
66			997	958	23.64	0.32	$\delta_{C1C2C6(14)}$
67			991	952	4.86	1.15	$\tau_{H27C11C8C9(55)}$
68			989	950	12.39	1.72	$\tau_{H27C11C8C9(22)}$
69			962	924	4.68	0.58	$\tau_{H27C11C8C9(72)}$

Table 2 (Cont) Comparison of the experimental and calculated vibrational spectra and proposed assignments of Ketotifen

70	**903**	**912**	**944**	**907**	**5.98**	**1.05**	**$\nu_{C20C21(26)}$**
71	875		935	898	11.09	0.40	$\tau_{C6C7C8C9(14)}$
72	870		906	871	2.43	1.14	$\tau_{H23C3C4H24(63)}$
73			898	863	1.22	0.35	$\tau_{H27C11C8C9(31)}$
74		852	884	850	2.03	2.21	$\tau_{H27C11C8C9(37)}$
75			863	829	20.32	1.22	$\nu_{S5C4(42)}+\delta_{C2C3C4(18)}$
76			849	816	2.02	4.31	$\nu_{C8C9(45)}+\delta_{C12C13C14(16)}$
77			844	811	1.39	0.75	$\nu_{N16C17(11)}+\tau_{H32C17N16C22(11)}+\gamma_{C18C17C19H33(21)}$
78			806	774	5.95	0.20	$\nu_{S5C4(18)}+\tau_{H27C11C8C9(10)}$
79			770	740	23.95	2.22	$\tau_{H27C11C8C9(65)}$
80			767	737	5.58	11.74	$\nu_{N16C17(51)}+\tau_{H27C11C8C9(11)}$
81			761	731	21.95	3.23	$\nu_{C18C19(10)}+\tau_{H23C3C4S5(38)}$
82		714	744	714	5.78	3.15	$\nu_{C18C19(11)}+\delta_{C2C3C4(11)}+\tau_{C11C8C7C14(20)}$
83			715	687	14.43	7.45	$\tau_{H23C3C4S5(30)}$
84	670		709	681	4.17	10.84	$\nu_{S5C4(12)}+\delta_{C1S5C4(12)}$
85			683	656	13.13	3.25	$\delta_{C11C12C13(15)}+\tau_{C1C2C3C4(13)}$
86		632	670	644	1.84	1.75	$\delta_{C1S5C4(12)}$
87	606		634	609	1.52	2.06	$\tau_{C1C2C3C4(24)}$
88			610	586	14.07	1.28	$\delta_{C9C8C11(28)}$
89	554	552	586	563	4.11	4.58	$\delta_{C17C18C19(18)}$
90			556	534	1.41	1.90	$\tau_{C11C12C13C14(22)}$
91			541	520	4.85	7.58	$\delta_{C18C17N16(15)}$
92			534	513	5.91	3.24	$\delta_{C17N16C21(17)}+\tau_{C11C12C13C14(10)}+\gamma_{C6C8C14C7(13)}$
93		476	498	478	0.89	5.30	$\nu_{C1C2(14)}+\delta_{C2C1C10(17)}$
94	468		477	459	3.57	4.42	$\tau_{C1S5C4C3(21)}$
95		443	455	437	0.60	1.90	$\delta_{C1S5C4(15)}+\tau_{C8C7C14C13(26)}$
96			452	435	1.93	7.05	$\tau_{C1S5C4C3(51)}+\tau_{C1S5C4C3(51)}$
97			420	403	1.61	4.10	$\delta_{C6C19C18(10)}+\tau_{H35C20C19C18(10)}$
98			410	394	1.00	1.68	$\delta_{C6C19C18(29)}$
99		355	391	376	3.04	2.85	$\delta_{C9C8C11(35)}$
100			343	330	1.44	3.15	$\delta_{C1C2C6(11)}+\tau_{C8C7C14C13(13)}$
101			321	308	2.44	2.31	$\tau_{C6C19C18C17(18)}+\gamma_{C22C17C21N16(29)}$
102			317	304	1.63	2.88	$\nu_{C2C3(14)}+\tau_{C8C7C14C13(10)}$
103			306	294	0.35	3.63	$\delta_{C6C19C18(19)}$
104			290	278	2.86	1.42	$\delta_{C18C17N16(14)}+\tau_{C19C18C17N16(17)}$
105			253	243	4.10	10.20	$\delta_{C3C2C6(21)}$
106			249	239	0.64	4.47	$\tau_{H39C22N16C21(23)}+\gamma_{C3C1C6C2(16)}$
107			230	221	0.94	1.26	$\tau_{H39C22N16C21(56)}$
108			218	210	1.52	3.14	$\delta_{C3C2C6(14)}$
109		173	162	156	0.49	23.74	$\tau_{C11C8C7C14(22)}$
110			151	145	0.08	4.63	$\tau_{C6C2C1C10(42)}$
111			130	125	1.08	45.58	$\tau_{C6C19C18C17(20)}+\gamma_{C6C8C14C7(13)}$
112		83	87	83	1.53	10.16	$\tau_{C1C10C9C8(43)}$
113			80	77	0.02	57.35	$\delta_{C7C6C19(25)}+\gamma_{C6C8C14C7(18)}$
114			76	73	0.27	5.30	$\tau_{C7C6C19C18(61)}$
115			68	65	0.16	77.99	$\delta_{C2C6C7(19)}+\gamma_{C3C1C6C2(42)}$
116			51	49	1.17	64.77	$\delta_{C7C6C19(13)}+\tau_{C1C10C9C8(11)}+\gamma_{C6C8C14C7(40)}$
117			21	20	0.95	100.00	$\tau_{C6C19C18C17(80)}$

v- Stretching; δ-in-plane-bending; γ-out-of-plane bending; τ- torsion; w- weak; s- strong; vs- very strong; vw- very weak; m- medium.
[a]I_{IR}- IR Intensity (Kmmol^{-1});
[b]I_{Ra}- Raman intensity (Arb units) (intensity normalized to 100%)

Natural bond orbital analysis

The natural bond orbital analysis provides an efficient method for studying intra-and intermolecular bonding and interaction among bonds, and also provides a convenient basis for investigating charge transfer or conjugative interaction in molecular systems; it could enhance the analysis of the delocalization of charge in the system. The donor bonding orbitals, the acceptor antibonding orbitals, the donor lone pair atoms are given in Table. 3 along with the E (2) values which estimates the interaction between the donor (filled) and acceptor (vacant) orbitals [22]. The E (2) energy is the lowering energy that occurs during the hyper conjugative electron transfer process and hence E (2) can be referred to as stabilization energy.

Larger the E (2) values, greater is the stability of the molecule. In the NBO analysis of the compound KT, the E (2) values are greater for the delocalization of the electrons between the bonds present in the Benzoic ring. For each donor NBO (i) and acceptor NBO (j); the stabilization energy E associated with i→j delocalization, is explicitly estimated by the following equation:

$$E_2 = \Delta E_{ij} = q_i \frac{F(i,j)^2}{\text{£}_j - \text{£}_i}$$

Where q_i is the donor orbital occupancy, are ε_i and ε_j diagonal elements and F(i,j) is the off diagonal NBO Fock matrix element.

The interactions π(C1-C2) → π*(C3-C4) and π*(C10-O15) having the stabilization energy is 14.70, 22.22 KJ mol^{-1} , π(C3-C4) → π*(C1-C2) having the stabilization energy is 16.76 KJ mol^{-1} are responsible for conjugation of respective π-bonds in Thiophen ring (Table 3). π(C7-C14) →π*(C8-C11) and π*(C12-C13) having the stabilization energy is 20.46, 20.63 KJ mol^{-1}. π(C8-C11) → π*(C7-C14) and π*(C12-C13) having energy is 20.60, 20.64 KJ mol^{-1}. π(C12-C13) → π*(C7-C14) and π*(C8-C11) having the stabilization energy is 20.32, 20.05 KJ mol^{-1} are responsible for conjugation of respective π-bonds in Benzoic ring. The energy contribution of LP (1)O15→ σ*(C1-C10) and σ*(C4-S5) are 19.09, 21.00 KJ mol^{-1} respectively.

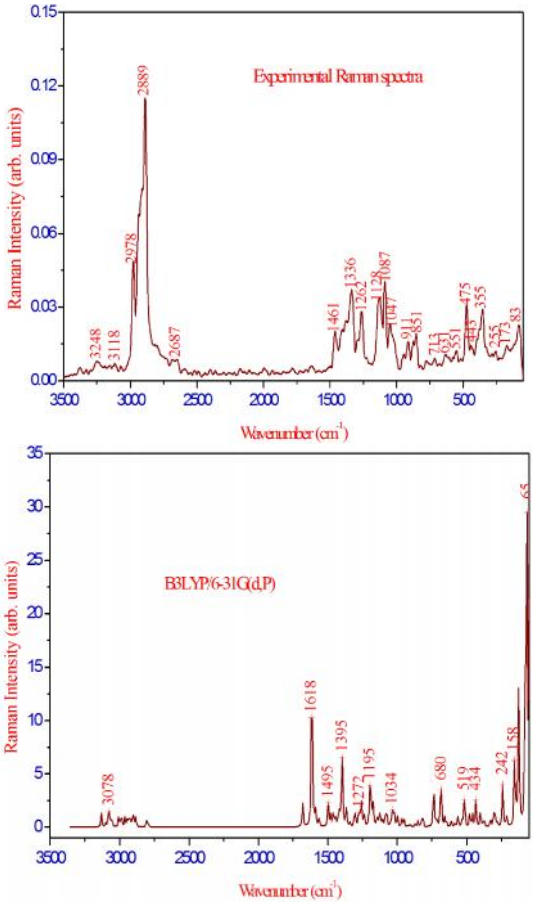

Fig.3 Comparison of experimental and theoretical B3LYP/6-31G(d,p) FT-Raman spectrum for Ketotifen

Electronic properties

UV-Visible spectral analysis

The experimental UV–Visible electronic absorption maxima *(λmax)* of Ketotifen recorded in ethanol together with the theoretical results involving the vertical excitation energies, oscillator strength (f) and wavelength at maximum absorption calculated at B3LYP/ 6-31G(d,p) basis set in gas phase and in ethanol solvent are given in Table 4. The experimental UV-Vis spectrum of the title compound is shown in Fig. 4. Due to the Frank–Condon principle, the maximum absorption peak (λmax) in an UV–visible spectrum corresponds to vertical excitation. The B3LYP/6-31G(d,p) calculations (in ethanol) predict two intense electronic transitions at 3.4975 eV (354.50 nm) with an oscillator strength f = 0.0070 and other one 3.7871 eV (327.39 nm) with an oscillator strength f = 0.1284, which are in good agreement with the measured experimental data (278 and 207 nm).

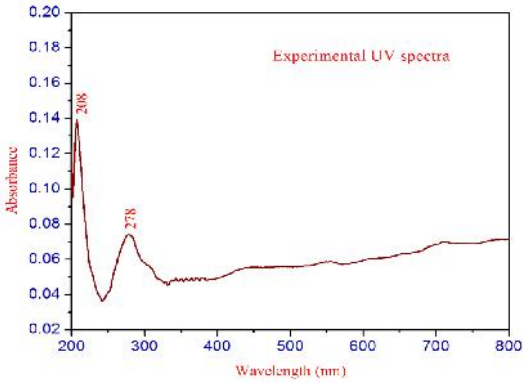

Fig.4 UV-Visible spectrum (Ethanol) of Ketotifen

Homo-Lumo Analysis

Molecular orbitals, when viewed in a qualitative graphical representation, can provide insight into the nature of reactivity, and some of the structural and physical properties of molecules. Both the highest occupied molecular orbital (HOMO) and lowest unoccupied molecular orbital (LUMO) are the main orbitals taking part in chemical reactions. The HOMO energy characterizes the ability of electron donating; LUMO characterizes the ability of electron accepting and the gap between HOMO and LUMO characterizes the molecular chemical stability.

Table 3 Second order Perturbation theory analysis of Fock Matrix in NBO basis for Ketotifen

Donor (i)	E_D (i)(e)	Acceptor(j)	E_D (j)(e)	E(2)[a] KJ mol^{-1}	E(j)-E(i)[b] a.u	F(i,j)[c] a.u
π(C1-C2)	1.773	π*(C3-C4)	0.293	14.70	0.28	0.058
π(C1-C2)	1.773	π*(C10-O15)	0.173	22.22	0.29	0.073
π(C3-C4)	1.837	π*(C1-C2)	0.370	16.76	0.30	0.067
π(C7-C14)	1.661	π*(C8-C11)	0.342	20.46	0.28	0.068
π(C7-C14)	1.661	π*(C12-C13)	0.334	20.63	0.28	0.068
π(C8-C11)	1.657	π*(C7-C14)	0.347	20.60	0.28	0.068
π(C8-C11)	1.657	π*(C12-C13)	0.334	20.64	0.28	0.068
π(C12-C13)	1.663	π*(C7-C14)	0.347	20.32	0.28	0.068
π(C12-C13)	1.663	π*(C8-C11)	0.342	20.05	0.29	0.068
LP(2)S5	1.603	π*(C1-C2)	0.370	20.43	0.27	0.066
LP(2)S5	1.603	π*(C3-C4)	0.293	23.87	0.26	0.072
LP(1)O15	1.976	RY*(1)C10	0.017	15.16	1.49	0.134
LP(2)O15	1.882	σ*(C1-C10)	0.063	19.09	0.72	0.106
LP(2)O15	1.882	σ*(C4-S5)	0.019	21.00	0.63	0.104
π*(C1-C2)	0.370	π*(C6-C19)	0.106	15.25	0.05	0.052

Energy difference between HOMO and LUMO orbital is called as energy gap that is an important stability for structures [23]. The energy gap is largely responsible for the chemical and spectroscopic properties of the molecules.

Table 4 The experimental and computed absorption wavelength λ (nm), excitation energies E (eV), absorbance and oscillator strengths (*f*) of Ketotifen in Ethanol solution and gas phase.

Experimental		**TD-DFT/B3LYP/6-31G(d,p)**					
Ethanol		**Ethanol**			**Gas**		
λ(nm)	Abs.	λ(nm)	E(eV)	f(a.u)	λ(nm)	E(eV)	f(a.u)
		398.21	3.1136	0.0027	373.41	3.3203	0.0018
278	0.0742	354.50	3.4975	0.0275	360.20	3.4421	0.0070
207	0.1392	327.39	3.7871	0.1349	312.49	3.9676	0.1284

This also used by the frontier electron density for predicting the most reactive position in p-electron systems and also explains several types of reactions in conjugated systems [24]. From the plots we can see that the region of HOMO and LUMO levels spread over the entire molecule and the calculated energy gap of HOMO–LUMO's explains the ultimate charge transfer interface within the molecule. The title molecule is given in Fig. 5. In addition, according to B3LYP/6-31G(d,p) calculation, the energy band gap of the NPBS molecule is 5.2149 eV shown in Fig. 6. The positive and negative phase is represented in red and green color, respectively.
HOMO energy = -5.5487eV
LUMO energy = -1.7589 eV
HOMO-LUMO energy gap = 3.7898 eV

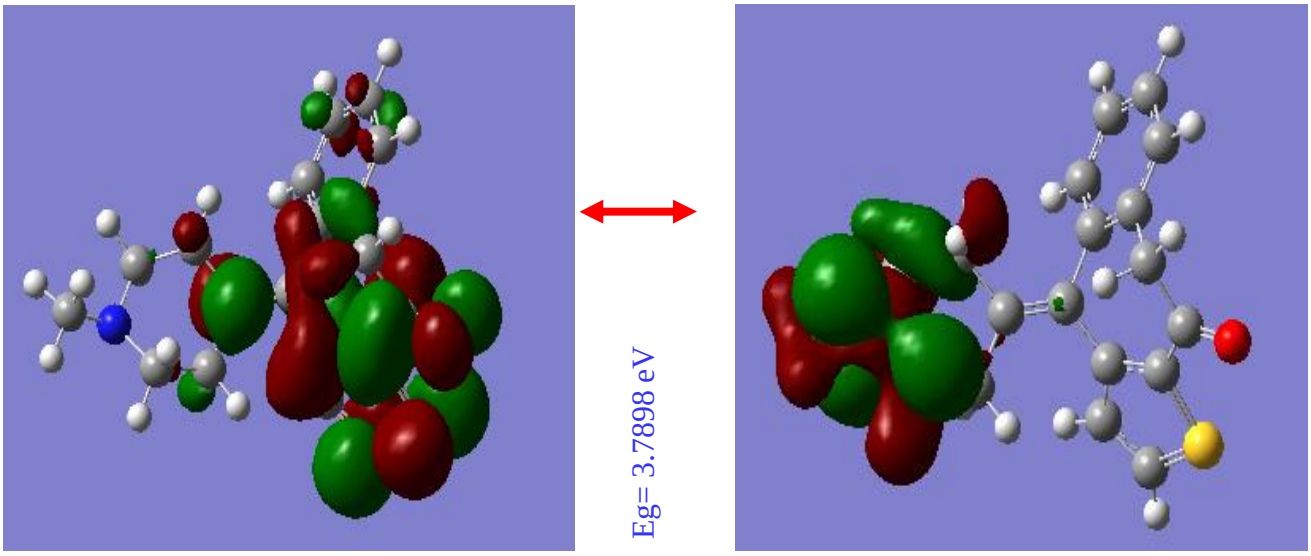

LUMO = -1.7589 eV HOMO = -5.5487eV

Fig.5 The atomic orbital compositions of the frontier molecular orbital for Ketotifen

Molecular Electrostatic Potential (MEP) Analysis

In order to grasp the molecular interactions, the molecular electrostatic potentials (MEPs) are used. Recently, the MEPs have been used for interpreting and predicting relative reactivities sites for eletrophilic and nucleophilic attack, investigation of biological recognition, hydrogen bonding interactions, studies of molecular cluster, crystal behavior, correlation and prediction of a wide range of macroscopic properties [25]. The MEP diagram (front and back view) of the Ketotifen molecule is shown in Fig.6. The color scheme for the MEP surface will be partially negative charge or maybe red-electron rich; partially positive charge or maybe blue-electron deficient; yellow slightly electron packed region; light blue-slightly electron deficient region, Additionally, green color parts represent also regions of zero potential respectively. For the title molecule yellow color represents the electron packed region which is mostly cover the oxygen atoms and also the positive region is actually over the NH group. Green color represents the zero potential regions mostly over the all protons.

Molecular Docking studies

Molecular docking studies were performed to investigate the binding affinities of the newly compound Ketotifen and the human asthma protein [1ZMS]. The title molecule is given in Fig. 7 and the values are tabulated in Table 5. The ligand-protein complex stability was successfully made by some features such as hydrogen bond interactions, vander Waals forces, $\pi \rightarrow \pi$ stacking interactions, hydrophobic interactions. These interactions between the drug and receptor depend upon the nature of functional groups present in the ligand.

On ligand preparation (by ligprep module) of compound KT structures were obtained. Water molecules and co-crystallized ligands were removed. Molecular docking studies were performed to investigate the higher binding affinities and total intermol energy of the newly compound Ketotifen is -5.49 kcal/ mol and -5.79 kcal/ mol lower binding affinities and total intermol energy of the title molecules is -4.80 kcal/ mol and -5.10 kcal/ mol respectively.

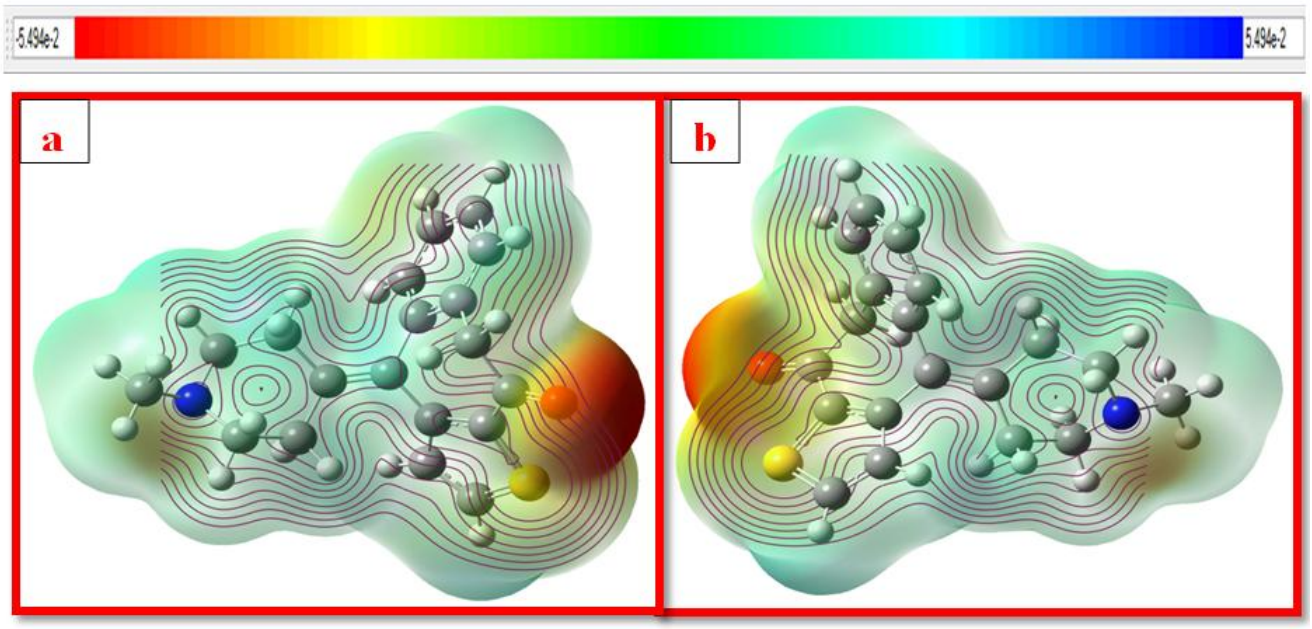

Fig.6. a Front view b) back view of Molecular electrostatic Potential map (MEP) for Ketotifen

Table. 5 Comparison of Est. Free Energy of Binding, Total Intermol. Energy of Ketotifen

Mode	Est. Free Energy of Binding	Total Intermol. Energy
1	-5.49 kcal/ mol	-5.79 kcal/ mol
2	-5.30 kcal/ mol	-5.59 kcal/ mol
3	-5.28 kcal/ mol	-5.58 kcal/ mol
4	-5.08 kcal/ mol	-5.38 kcal/ mol
5	-4.80 kcal/ mol	-5.10 kcal/ mol

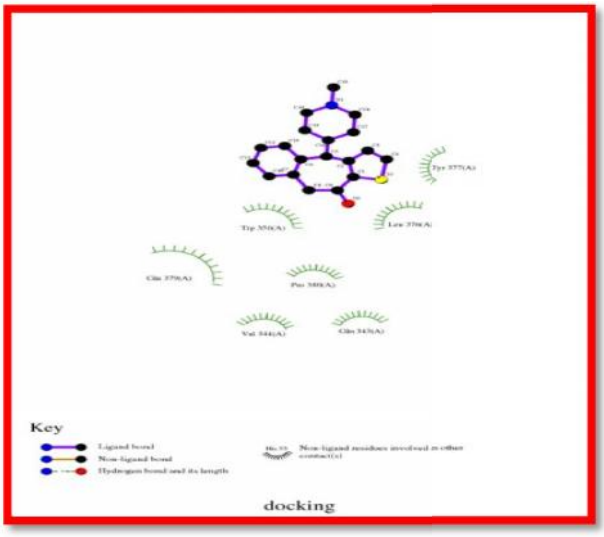

(A)

Fig.7 (A) 2D docking poses of compound ketotifen (protein with ligand)

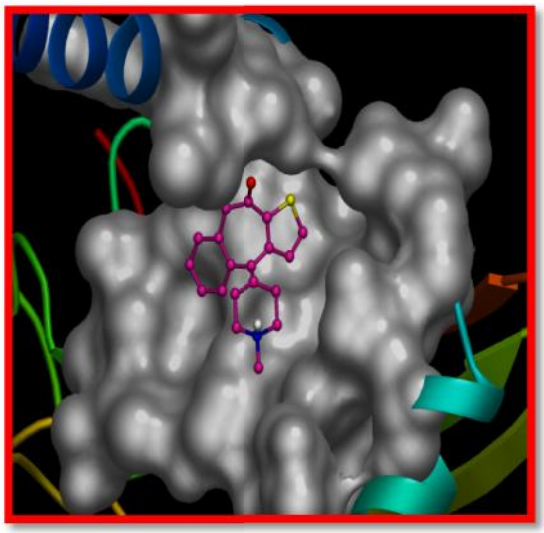

(B)

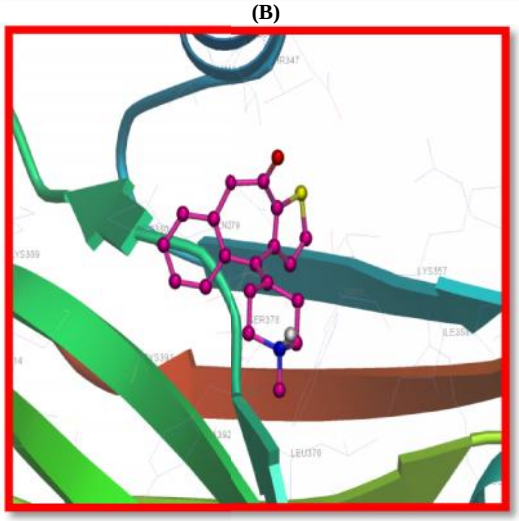

Fig.7 (B, C) 3D docking poses of compound ketotifen (protein with ligand)

CONCLUSION

A novel compound Ketotifen was characterized by FT-IR, FT-Raman, UV techniques. The theoretical vibrational frequencies are found to be in good agreement with the observed vibrational frequencies of title molecules**.** The compound Ketotifen is subjected to NBO analysis, the E (2) values are greater for the delocalization of the electrons between the bonds present in the thiophen ring. Moreover, frontier molecular orbitals and molecular electrostatic potential were visualized. Electronic transition and energy band gap of the title molecule were investigated and interpreted. The title molecular HOMO-LUMO energy gap is 3.7898 eV. The molecular docking of the compound shows the various interactions between the ligand and protein active respectively.

References

1. Grant, S. M., Goa, K. L., Fitton, A., & Sorkin, E. M. Ketotifen: A review of its Pharmacodynamic and pharmacokinetic properties, and therapeutic use in asthma and allergic disorders. Drugs, 40 **(**1990) 412–448.
2. Sandra Guerrero, Cesar Teijon, Enriqueta Muniz, Jose M. Teijon, M. Dolores Blanco ‟Characterization and in vivo evaluation of ketotifen-loaded chitosan microspheres" Carbohydrate Polymers 79 (2010) 1006–1013.
3. Gaussian Inc., Gaussian 03 Program, Gaussian Inc., Wallingford, (2004).
4. H.B. Schlegel, J. Comput. Chem. 3 (1982) 214–218.
5. A. Frisch, A.B. Nielson, A.J. Holder, Gauss view User Manual, Gaussian Inc., Pittsburgh, PA, (2000).
6. M.H. Jamroz, Vibrational Energy Distribution Analysis VEDA 4, Warsaw, (2004).
7. N.C. Handy, P.E. Maslen, R.D. Amos, J. Phys. Chem. 97 (1993) 4392–4396.
8. V. Krishnakumar, R. Mathammal, S. Muthunatesan, Spectrochim. Acta 70A (2008) 210–216.
9. E.D. Glendening, A.E. Reed, J.E. Carpenter, F. Weinhold, NBO Version3.1, TCI, University of Wisconsin, Madison, (1998).
10. L. E. Sutton, ‟Tables of Interatomic Distances, Chemical Society", London, (1958).
11. R. Solaichamy, J. Karpagam, ‟Structural and Vibrational studies (FT-IR, FT-Raman) of Voglibose using DFT calculation", International Letters of Chemistry, Physics and Astronomy 64 (2016) 45–62.
12. http://www.rcsb.org/pdb/explore.do?structureId=2zq1.
13. M.F. Sanner, J. Mol. Graph. Model. 17 (1999) 57–61.
14. A.A. Adeniyi, P.A. Ajibade, J. Mol. Graph. Model. 38 (2012) 60–69.
15. http:// www.clcbio.com/products/molegro/.
16. Mansuy, D., Valadon, P., Erdelmeier, I., Lopez-Garcia, P., Amar, C., Girault, J. P., and Dansette, P. M. ‟Thiophene S-oxides as new reactive metabolites: Formation by cytochrome-P450 dependent oxidation and reaction with nucleophiles". J. Am. Chem. Soc. 113 (20) (1991) 7825–7826.
17. Treiber, A., Dansette, P.M., Amri, H.E., Girault, J.-P., Ginderow, D., Mornon, J.-P., Mansuy, D.; Dansette; El Amri; Girault; Ginderow; Mornon; Mansuy. ‟Chemical and Biological Oxidation of Thiophene: Preparation and Complete Characterization of Thiophene S-Oxide Dimers and Evidence for Thiophene S-Oxide as an Intermediate in Thiophene Metabolism in Vivo and in Vitro". J. Am. Chem. Soc. 119 (1997) 1565–1571.
18. Alexander J. Blake ‟Intramolecular and intermolecular geometry of thiophenes with oxygen-containing substituent's Acta Cryst. (1999) 963-974.
19. D. Sajan, J. Binoy, B. Pradeep, K.V. Krishnan, V.B. Kartha, I.H. Joe, V.S. Jayakumar, ‟NIR-FT Raman and infrared spectra and ab initio computations of glycinium oxalate" Spectrochim. Acta A60 (2004) 173.
20. N.B.Colthup, L.H.Daly, S.E.Wiberly, ‟Introduction to Infrared and Raman Spectroscopy", 3rd ed., Academic Press, Boston (1990).
21. R.M. Silverstein, G.C. Bassler, T.C.Morril, ‟Spectrometric Identification of Organic Compounds", ed. 5, John Wiley and Sons, Inc., Singapore (1991).
22. A.E. Reed, L.A. Curtiss, F. Weinhold, ‟Intermolecular Interactions from a Natural Bond Orbital, Donor-Acceptor Viewpoint," Chem. Rev. 88 (1988) 899–926.
23. F.V. Lewis, C. Ioannides, D.V. Parke, Xenobiotica 24 (1994) 401–408.
24. K. Govindarasu, E. Kavitha, Spectrochim. Acta A 133 (2014) 417–431.
25. J.S. Murray, K.Sen, ‟Molecular Electrostatic Potential Concepts and Applications, Elsevier Science" B.V, Amsterdaam, The Netherlands (1996).

****

How to cite this article:

Solaichamy R and Karpagam J.2016, Molecular Structure, Molecular Docking, Molecular Structure, Molecular Docking, Vibrational Spectra, Nbo, and Uv-Visible Analysis of Ketotifen by Dft Method. *Int J Recent Sci Res.* 7(4), pp. 9840-9849.

TSSN 0976-3031